

# Circulation Research

JOURNAL OF THE AMERICAN HEART ASSOCIATION

American Heart  
Association®   
*Learn and Live*<sup>SM</sup>

## **The Hydrodynamically Relevant Endothelial Cell Glycocalyx Observed In Vivo Is Absent In Vitro**

Daniel R. Potter and Edward R. Damiano

*Circ. Res.* 2008;102;770-776; originally published online Feb 7, 2008;

DOI: 10.1161/CIRCRESAHA.107.160226

Circulation Research is published by the American Heart Association, 7272 Greenville Avenue, Dallas, TX 75214

Copyright © 2008 American Heart Association. All rights reserved. Print ISSN: 0009-7330. Online ISSN: 1524-4571

The online version of this article, along with updated information and services, is located on the World Wide Web at:

<http://circres.ahajournals.org/cgi/content/full/102/7/770>

Subscriptions: Information about subscribing to Circulation Research is online at  
<http://circres.ahajournals.org/subscriptions/>

Permissions: Permissions & Rights Desk, Lippincott Williams & Wilkins, a division of Wolters Kluwer Health, 351 West Camden Street, Baltimore, MD 21202-2436. Phone: 410-528-4050. Fax: 410-528-8550. E-mail:  
[journalpermissions@lww.com](mailto:journalpermissions@lww.com)

Reprints: Information about reprints can be found online at  
<http://www.lww.com/reprints>

## The Hydrodynamically Relevant Endothelial Cell Glycocalyx Observed In Vivo Is Absent In Vitro

Daniel R. Potter, Edward R. Damiano

**Abstract**—In recent years, the endothelial cell surface glycocalyx has emerged as a structure of fundamental importance to a broad range of phenomena that determine cardiovascular health and disease. This new understanding of the functional significance of the glycocalyx has been made possible through recently developed experimental techniques using intravital microscopy that are capable of directly probing the glycocalyx in vivo. Using fluorescent microparticle image velocimetry in venules and endothelialized cylindrical collagen microchannels, we show that the hydrodynamically relevant endothelial cell glycocalyx surface layer observed in microvessels in vivo ( $0.52 \pm 0.28 \mu\text{m}$  thickness), which is a fundamental determinant of the hydrodynamic and mechanical environment at the endothelial cell surface, is absent from human umbilical vein ( $0.03 \pm 0.04 \mu\text{m}$  thickness) and bovine aortic ( $0.02 \pm 0.04 \mu\text{m}$  thickness) endothelial cells grown and maintained under standard cell culture conditions in vitro. An endothelial surface-bound glycosaminoglycan layer, not necessarily indicative of but having similar hydrodynamic properties to the endothelial glycocalyx observed in vivo, was detected ( $0.21 \pm 0.27 \mu\text{m}$  thickness) only after hyaluronan and chondroitin sulfate were added to the cell culture media at hyperphysiological concentrations (0.2 mg/mL perfused for 75 minutes). The implications of this glycocalyx deficiency under standard cell culture conditions in these pervasive in vitro models broadly impact a myriad of studies involving endothelial cell monolayers in which inferences are made that may depend on endothelial cell surface chemistry. In light of these findings, conclusions drawn from such studies in the areas of microvascular permeability, inflammation, mechanotransduction, and atherosclerosis must be carefully reconsidered. (*Circ Res.* 2008;102:770-776.)

**Key Words:** cell culture ■ glycocalyx ■ mechanotransduction ■ microcirculation ■ vascular inflammation ■ vascular permeability

Numerous studies of endothelial cells (ECs) in culture have been undertaken in recent years that are intended to elucidate mechanisms of EC function spanning a broad range of fields in cardiovascular physiology and pathophysiology, including inflammation, vascular permeability, EC mechanotransduction, and atherosclerosis.<sup>1-9</sup> The scientific utility of these and many other studies involving ECs in culture is often critically dependent on cultured systems bearing close morphological, structural, and functional similarities to the tissues they are designed to emulate. Whether or not acknowledged, cell surface chemistry and, specifically, the state of the EC surface glycocalyx in vitro, is a fundamental determinant of the outcome of many of these studies.

Over the past decade, it has become well established that the EC surface glycocalyx, a membrane-bound layer of carbohydrates and adsorbed plasma proteins, previously thought to be less than  $\approx 50$  nm in thickness, in fact extends  $\approx 500$  nm from the surface of the vascular endothelium in vivo.<sup>10-13</sup> Vink and Duling<sup>10</sup> first showed this in hamster cremaster muscle capillaries in vivo using a dye-exclusion method. Later, microparticle image velocimetry ( $\mu$ -PIV) was

used<sup>11,12</sup> in mouse cremaster muscle venules in vivo to show that hydrodynamic drag within the glycocalyx resulted in nearly complete cessation of plasma flow within  $\approx 500$  nm of the vessel wall. To reconcile these experimental observations with our understanding of the rheological properties of blood and its cellular constituents, various theoretical studies<sup>14-22</sup> have been undertaken in recent years to characterize the mechanical properties and dynamical behavior of the endothelial glycocalyx in vivo. It is through these experimental and theoretical investigations that a new understanding has emerged of the many functional roles of the endothelial glycocalyx in cardiovascular health and disease. In particular, the fact that the intact glycocalyx is stiff enough<sup>17-19</sup> to prevent red and white blood cells from approaching unflamed endothelium in postcapillary venules has required revision of conventionally held views regarding leukocyte capture and the initiation of the inflammatory response cascade in vivo.<sup>11,23-28</sup> Furthermore, the fact that the glycocalyx essentially eliminates fluid shear stress on the EC surface has required a reinterpretation of popular views on stress transmission to vascular endothelium and mechanisms

Original received July 18, 2007; revision received January 26, 2008; accepted January 30, 2008.

From the Department of Biomedical Engineering, Boston University, Mass.

Correspondence to Edward R. Damiano, Associate Professor of Biomedical Engineering, Boston University, Biomedical Engineering, 44 Cummington St, Boston, MA 02215. E-mail edamiano@bu.edu

© 2008 American Heart Association, Inc.

Circulation Research is available at <http://circres.ahajournals.org>

DOI: 10.1161/CIRCRESAHA.107.160226

of EC mechanotransduction.<sup>7,8,14,18,20,29</sup> In addition, the fact that the glycocalyx completely retards plasma flow near the EC surface has suggested a role for the layer in vascular permeability to water and macromolecules.<sup>10,30,31</sup>

It was not until the dye-exclusion technique developed by Vink and Duling<sup>10</sup> that the true extent of the EC glycocalyx was first discovered *in vivo*. Recent attempts at visualizing the glycocalyx have relied on electron microscopic imaging,<sup>30–33</sup> which typically required either dehydration of the extracellular matrix before tissue fixation or other fixation procedures. Because the fluid volume fraction of the glycocalyx is very near unity,<sup>34</sup> many fixation attempts resulted in a partial collapse of the charged mucopolysaccharide structures in the glycocalyx, which left behind a remnant of the layer that was typically only 20 to 50 nm in thickness. For the same reason, *in vivo* imaging of the glycocalyx using bright field microscopy also presents a challenge because the preponderance of glycocalyx volume consists of blood plasma and therefore has an optical refractive index that is too close to the surrounding blood to distinguish its luminal boundary. Using both bright field and fluorescence microscopy on mouse cremaster muscle capillaries *in vivo*, Vink and Duling<sup>10</sup> were able to show that 70-kDa fluorescein isothiocyanate (FITC)-dextran plasma tracers were sterically excluded by the glycocalyx and that the diameter of the resulting FITC-dextran dye column was  $\approx 0.8$ – $1\ \mu\text{m}$  smaller than the anatomic diameter of the capillary, as measured under bright field illumination. They also suggested that oxygen-derived free radicals were generated during epifluorescent illumination of the FITC-dextran column within the microvessel and caused shedding of the glycocalyx and that this light-dye treatment was substantially blocked in the presence of exogenous free radical scavengers.

The utility of the dye-exclusion technique is limited to microvessels less than  $\approx 15\ \mu\text{m}$  in diameter because of optical difficulties associated with focusing on the boundary of the FITC-dextran column in larger microvessels.<sup>35</sup> To address this limitation, Damiano and coworkers used  $\mu$ -PIV to interrogate the endothelial glycocalyx in microvessels more than  $\approx 20\ \mu\text{m}$  in diameter.<sup>11–13</sup> The method extracts the velocity field within a microvessel based on simultaneous measurements of the velocity and radial position of individual 500-nm-diameter fluorescent polystyrene microspheres flowing in a microvessel. Because of the asymmetrical distribution of the hydrodynamic drag force over the surface of microspheres near the vessel wall, the local 3D fluid dynamics is analyzed in the neighborhood of each microsphere and is used to estimate the near-wall velocity profile that would arise in the absence of the microspheres. Application of this method to blood flow in mouse cremaster muscle venules ( $\approx 20$  to  $50\ \mu\text{m}$  in diameter) *in vivo* revealed a highly nonlinear velocity profile within  $\approx 500\ \text{nm}$  of the vessel wall,<sup>12,13</sup> which is suggestive of a non-Newtonian source of hydrodynamic drag on the plasma permeating through the fiber matrix of the glycocalyx throughout this region. In essence, the presence of an intact glycocalyx gives the appearance that the fluid velocity in the vessel lumen vanishes at a radial location that is  $\approx 500\ \text{nm}$  away from the EC surface rather than at the EC surface. These measurements

provided direct evidence that the hydrodynamically relevant portion of the glycocalyx (in the sense of retarding plasma flow) extends as far from the surface of the vascular endothelium in venules  $>20\ \mu\text{m}$  in diameter as the dye-exclusion region does in capillaries and microvessels  $<15\ \mu\text{m}$  in diameter.<sup>10,12,13,35</sup> It was further shown using this technique that the hydrodynamically relevant glycocalyx thickness was reduced to  $\approx 200\ \text{nm}$  after light-dye treatment to degrade the glycocalyx.<sup>12</sup>

To test the status of the EC glycocalyx *in vitro*, we have sought to determine whether a hydrodynamically relevant glycocalyx is present on ECs grown to confluence under physiologically typical flow using standard cell culture conditions. Any attempt at visualizing the glycocalyx on cultured ECs *in vitro* using a traditional flow chamber is inherently limited by the fact that such systems do not typically afford a side view of the EC. Such a perspective is necessary, however, if either dye exclusion or  $\mu$ -PIV is to be used to interrogate the glycocalyx *in vitro*. We have therefore used  $\mu$ -PIV in cylindrical collagen microchannels steadily perfused with cell culture media and lined on their luminal surface with a confluent monolayer of either human umbilical vein ECs (HUVECs) or bovine aortic ECs (BAECs). This flow chamber, developed by Chrobak et al.,<sup>36</sup> not only has the advantage of providing a side view of the EC monolayer under flow but also offers a biological extracellular matrix substrate (type I collagen) on which the cells are seeded and has a cylindrical geometry with a circular cross-section, similar to that of microvessels *in vivo*. Control experiments using  $\mu$ -PIV in mouse cremaster muscle venules were also performed using the same experimental approach.

## Materials and Methods

### Imaging and $\mu$ -PIV

$\mu$ -PIV was performed using a previously described technique.<sup>11–13</sup> Fluorescent microspheres were visualized using stroboscopic double-flash (1 to 9 ms apart, DPS-1 Video, Rapp Opto Electronic) epi-illumination on a Zeiss microscope (Axioskop II, Carl Zeiss Inc, Thornwood, NY), and recordings were made with a CCD camera (Sensicam QE, Cooke Inc) connected to a G5 Power Mac (Apple Inc). A Dualview (Optical Insights Inc) beam splitter separates infrared transillumination from the fluorescent microsphere image, allowing for simultaneous acquisition of the vessel or channel wall and the microspheres. The midsagittal plane was defined as corresponding to the focal plane at which the contrast of the edge of the intraluminal wall reversed.<sup>11</sup>

Images were captured and processed with IPlab (BD Biosciences) and analyzed with the public domain ImageJ program (<http://rsb.info.nih.gov/ij>) as described.<sup>11,37</sup> The flash-time interval for  $\mu$ -PIV recordings was chosen such that the 2 images for a given microsphere were  $\approx 3$  to  $10\ \mu\text{m}$  apart. The collagen microchannel data were collected with both  $40\times$  and  $63\times$  saline immersion objectives (NA, 0.8 and 1.0, respectively) to accurately capture both center-stream and near-wall microspheres. The distance between these 2 images and the shortest distance between the microsphere center and the vessel wall were measured for at least 40 microspheres in each venule or collagen microchannel. Because the velocity profile is known to be monotonically decreasing with increasing radial position, a microsphere in the midsagittal plane travels faster than any other microsphere at that measured radial location. In light of this, and considering that not all of the recorded microspheres travel in the midsagittal plane of the vessel, only the fastest microspheres at a given measured radial location were considered. As such, all  $\mu$ -PIV data sets were filtered to satisfy this monotonicity

condition as previously described.<sup>11,12</sup> Only monotonically filtered data were included in the analysis.

### Cell Culture

Human umbilical vein ECs (HUVECs) were cultured at 37°C in 5% CO<sub>2</sub> in medium 199 (Invitrogen) and supplemented with 1% L-glutamine (2 nmol/L), penicillin (100 U/mL), and streptomycin (100 µg/mL) (Invitrogen), 20% heat-inactivated FBS, 5 U/mL heparin (Sigma-Aldrich Co), and 25 µg/mL endothelial mitogen (ECGS, Biomedical Technologies). The cells were passaged with dispase (Fisher Scientific). Bovine aortic ECs (BAECs) were cultured at 37°C in 5% CO<sub>2</sub> in medium 199 (Invitrogen) and were supplemented with 2 nmol/L L-glutamine, 100 U/mL penicillin, 100 µg/mL streptomycin (1% GPS; Invitrogen), and 10% heat inactivated FBS. The cells were passaged with trypsin (Fisher Scientific). Both HUVECs and BAECs were cultured in gelatin-coated tissue culture dishes and discarded after passage 9.

### EC-Lined Collagen Microchannel Experiments

The flow chamber and in vitro culture system consist of an EC-lined cylindrical microchannel (with a circular cross section) through a collagen gel contained within a cured elastomer scaffold. Both ends of the microchannel were immersed in media reservoirs, which were connected via polyethylene tubing to culture dishes filled with media.

The microchannels are constantly perfused with media via a static gravity-induced pressure head. Culture media flows from the tissue culture dish feeding the microchannel to another culture dish, which collects the media and is located 5 cm below the feeding culture dish. At confluence the channels are ≈110 to 150 µm in diameter. The culture media is supplemented with 4% 70-kDa dextran to increase the viscosity of the media and thereby reduce the amount of media consumed. Between experiments, the channels remained in an incubator at 37°C in 5% CO<sub>2</sub>.

The µ-PIV data were collected for control experiments after Fluoresbrite YG microspheres (0.47±0.01 µm, ρ=1.05 g/cm<sup>3</sup>; Polysciences Inc, Warrington, Pa) were added to the culture media. The microchannels were thermocontrolled with the same superfusion apparatus used in the in vivo experiments. The superfusion solution was constantly pooled and aspirated away on the glass surface of the microchannel chamber and was either maintained at room temperature (23°C to 24°C) or thermocontrolled at body temperature (36°C to 38°C) with circulating water from a bath circulator (NESLAB EX-7 Digital One, Thermo Scientific). The temperature was measured before and after data collection with a digital thermometer. Data collection for a single collagen microchannel typically required 15 minutes. Following data collection for each control experiment, collagen microchannels were then treated with hyaluronidase (Sigma-Aldrich Co) by adding 100× stock hyaluronidase solution, prepared on the day of the experiment, to the reservoir, which provided a final hyaluronidase concentration of 50 U/mL. µ-PIV data were collected approximately 75 minutes after introducing the enzyme.

For experiments designed to constitute a glycosaminoglycan layer on ECs in vitro, 0.1 µg/mL hyaluronan (HA) (Sigma-Aldrich Co) and 0.1 µg/mL chondroitin sulfate (CS) (Sigma-Aldrich Co) were added to the culture media immediately after the HUVECs reached confluence. µ-PIV data were collected after 24 hours. The microchannels were then treated with hyaluronidase as described above. After enzyme treatment, µ-PIV data were again collected after which another bolus of HA and CS were added to the media, bringing the concentration of both glycosaminoglycans to 0.2 mg/mL (which is comparable to the pharmacological dose used by Henry and Duling<sup>35</sup> in their in vivo reconstitution experiments). After 75 minutes of perfusion, µ-PIV data were collected once again.

### Intravital Experiments

Intravital fluorescent µ-PIV methods and data analysis followed the in vitro protocols described above with variations noted below.

All animal experiments were conducted under a protocol approved by the Boston University Institutional Animal Care and Use Committee (protocol no. 2474). Wild-type male mice (C57Bl/6) were obtained from Charles River Laboratories (Wilmington, Mass). All mice appeared healthy and were between 8 and 14 weeks of age. The cremaster muscle was prepared for intravital microscopy as described.<sup>38</sup> Briefly, the cremaster muscle was exteriorized, pinned to the stage, and superfused with thermocontrolled bicarbonate-buffered saline equilibrated with 5% CO<sub>2</sub> in N<sub>2</sub> at either room temperature (23°C to 24°C) or body temperature (36°C to 38°C). This procedure was completed in 10 to 15 minutes.

As in the case of the collagen-microchannel experiments, intravital microscopic observations were made on a Zeiss microscope (Axioskop II, Carl Zeiss Inc, Thornwood, NY) with a 63× saline immersion objective (NA 1.0). A small volume (<0.03 mL) of fluorescent microspheres was slowly injected through the carotid cannula until 10 to 20 microspheres per second passed through the vessel. As in the case of the collagen microchannel experiments, Fluoresbrite YG microspheres were used in venules less than ≈40 µm in diameter. For larger-diameter venules, light scattering attributable to the red blood cells becomes more problematic. As such, Polychromatic red microspheres (0.513±0.015 µm, ρ=1.05 g/cm<sup>3</sup>; Polysciences Inc) were used for venules more than ≈40 µm in diameter. For venules more than ≈60 µm in diameter, Polychromatic red microspheres (1.75±0.055 µm, ρ=1.05 g/cm<sup>3</sup>; Polysciences Inc) were used in addition to the 0.47-µm-diameter Fluoresbrite YG microspheres. The 2 populations of microspheres were required to obtain full-field µ-PIV data, because the smaller-diameter microspheres could not be visualized near the center of these venules and the larger-diameter microspheres were too large to provide the resolution needed to account for the nonlinear shear rate distribution through the plasma-rich zone near the vessel wall. The larger microspheres were not counted if they were within 10 µm of the vessel wall. Measurements were not included if rolling or firmly adherent leukocytes were present anywhere within the 15-µm measurement window.

### Analytic Methods

The µ-PIV data presented here are interpreted using microviscometric analysis of blood flow in microvessels.<sup>12,13</sup> Microviscometric analysis invokes the continuum approximation and regards a heterogeneous red cell suspension as a homogeneous, continuously varying, linearly viscous incompressible fluid having a spatially nonuniform viscosity distribution over the vessel cross section. This approximation is reasonable for microvessels more than ≈20 µm in diameter.<sup>39</sup> It is further assumed that the velocity profile is axisymmetric and fully developed, which is reasonable for profiles in microvessels measured more than 1 vessel diameter away from bifurcations.<sup>40</sup> In cylindrical coordinates (*r*, θ, *z*), it can generally be shown<sup>12</sup> that for an axisymmetric, fully developed, steady flow of a purely viscous incompressible fluid having a radially variable dynamic viscosity, µ(*r*), in a rigid circular cylinder of radius *R*, the only nonvanishing viscous shear stress component, τ<sub>rz</sub>(*r*), varies linearly in absolute value from 0 at the tube center to a maximum at the tube wall. If, in particular, the constitutive relationship between the local shear rate, γ̇(*r*), and τ<sub>rz</sub>(*r*) is given by τ<sub>rz</sub>(*r*) = µ(*r*)γ̇(*r*), it can be shown<sup>12</sup> that

$$(1) \quad \tau_{rz}(r) = \frac{r}{a} \mu(a) \dot{\gamma}(a), \quad 0 < r < R$$

where *r*=*a* is the radial location corresponding to the interface between the endothelial glycocalyx and the fluid in the lumen. In the absence of a hydrodynamically relevant glycocalyx, *a*=*R*. In the case of a red cell suspension such as blood, µ(*a*) corresponds exactly to the viscosity of the blood plasma because the concentration of red blood cells at *r*=*a* vanishes.<sup>12,13</sup> All reported values of |τ<sub>max</sub>| were obtained by evaluating Equation 1 at *r*=*a* and noting that |τ<sub>max</sub>| = |τ(*a*)|. Thus, |τ<sub>max</sub>| = µ(*a*)|γ̇(*a*)| on 0 < *r* < *R*. All of these analytic results are valid in the special case of a Poiseuille flow in the lumen, such as was present in all of the EC-lined collagen microchannel

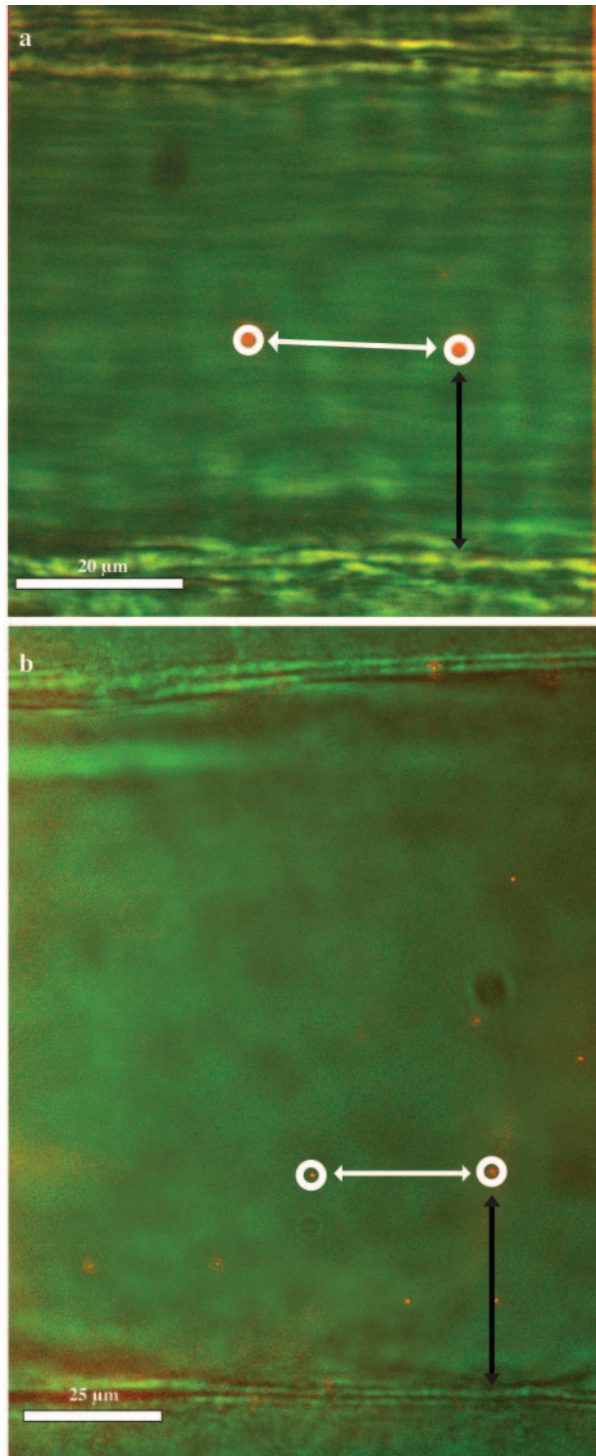


**Figure 1.** Image of a mouse cremaster muscle venule (a) and a HUVEC-lined collagen microchannel (b), each showing a double image of a fluorescent microsphere ( $\approx 0.5 \mu\text{m}$  diameter) being convected downstream. The images were obtained via simultaneous acquisition of the infrared transmission (green) and epifluorescent (red) light pathways. The epifluorescent pathway was illuminated by a fluorescent strobe that pulses twice during a single exposure, creating a double image of the fluorescent microsphere tracer in the fluid. Because the pulse interval is known and the flow is steady, the distance between the 2 images of the microsphere (white arrows) is indicative of the microsphere velocity. The distance to the venular EC surface (a) or HUVEC surface (b) is also measured (black arrows) to determine the radial position of the microsphere in the lumen.

experiments. This analysis has been tested and validated in mouse cremaster muscle venules in vivo (20 to 50  $\mu\text{m}$  in diameter) and in cylindrical glass tubes ( $\approx 50 \mu\text{m}$  in diameter) perfused with saline, blood plasma, and red cell suspensions in plasma.<sup>13</sup>

For in vivo experiments, the viscosity,  $\mu(a)$ , for blood plasma was taken to be 0.012  $\text{dyn/cm}^2$  at 37°C.<sup>12,13</sup> Viscosities of the perfusate solutions used in all EC-lined collagen microchannel experiments were measured at a variety of shear rates at 24°C using a cone-and-plate viscometer (DV-II+ Pro Programmable Viscometer, Brookfield Engineering Laboratories Inc.). For all in vitro experiments using standard cell culture conditions,  $\mu(a)$  was found to be 0.023  $\text{dyn/cm}^2$  while after a pharmacological dose of HA and CS was added to the culture media,  $\mu(a)$  was found to be 0.024  $\text{dyn/cm}^2$ .

The translational speed of the center of a microsphere very near the vessel/microchannel wall lags the velocity that a fluid particle would have at the same radial distance from the wall if the microsphere were not present in the flow. This was accounted for in the interpretation of the data. Following a previously described method,<sup>11</sup> the 3D analyses of the free motion of a neutrally buoyant sphere in a uniform shear field adjacent to a planar confining boundary<sup>41</sup> or a Brinkman half space<sup>42</sup> were used to infer, from the measured translational speed of the microsphere, the true fluid particle velocity that would arise in the absence of the particle tracer. The velocity profile over the vessel cross-section was extracted directly from the estimated fluid particle velocities rather than from the measured microsphere velocities.

### Statistical Analysis

Data were expressed as means  $\pm$  1 SD. The mean hydrodynamically relevant thickness of the EC surface layer for a given experimental group was considered statistically significantly different from 0 using a 1-sample 2-tailed  $t$  test, where a test of hypothesis showed that the mean layer thickness was significantly greater than 0  $\mu\text{m}$  if  $P < 0.05$ .

An expanded Materials and Methods section is in the online data supplement, available at <http://circres.ahajournals.org>.

### Results and Discussion

Figure 1 is representative of the images that were obtained in vivo and in vitro using double-strobe epifluorescence illumination. From such images,  $\mu$ -PIV data were extracted by measuring the translational speed and position (relative to the luminal EC surface) of all visible paired images of neutrally buoyant fluorescent microspheres convected by the flow. Representative velocity profiles, along with their corresponding shear rate distributions,  $\dot{\gamma} = dv_z/dr$ , are shown in Figure 2 superimposed on the  $\mu$ -PIV data obtained from 1 cremaster muscle venule and 1 collagen microchannel (additional results similar to Figure 2 are shown in Figures I through X in the online data supplement). The variation, relative to a trial glycocalyx thickness, in the normalized least-squares error,  $E^*$ , associated with the fit,  $\gamma_2(r)$ , to the  $\mu$ -PIV data (Figure 2) tracks the “quality” of the fit relative to each trial thickness. The minimum in this variation in  $E^*$  corresponds to the best fit of all trials and provides our calculated estimate for the hydrodynamically relevant thickness of the EC glycocalyx. In this way, each  $\mu$ -PIV data set, as in Figure 2, was analyzed to obtain an estimate of the hydrodynamically relevant glycocalyx thickness. All estimates of the hydrodynamically relevant glycocalyx thickness reported here were calculated using this approach. We found the mean hydrodynamically relevant glycocalyx thickness in cremaster muscle venules (45  $\pm$  20  $\mu\text{m}$ , 22 to 101  $\mu\text{m}$  diameter) to be  $0.52 \pm 0.28 \mu\text{m}$  (0.16 to 1.14  $\mu\text{m}$ ), which differs significantly from a thickness of 0  $\mu\text{m}$  ( $P < 0.0005$ ), whereas after hyaluronidase

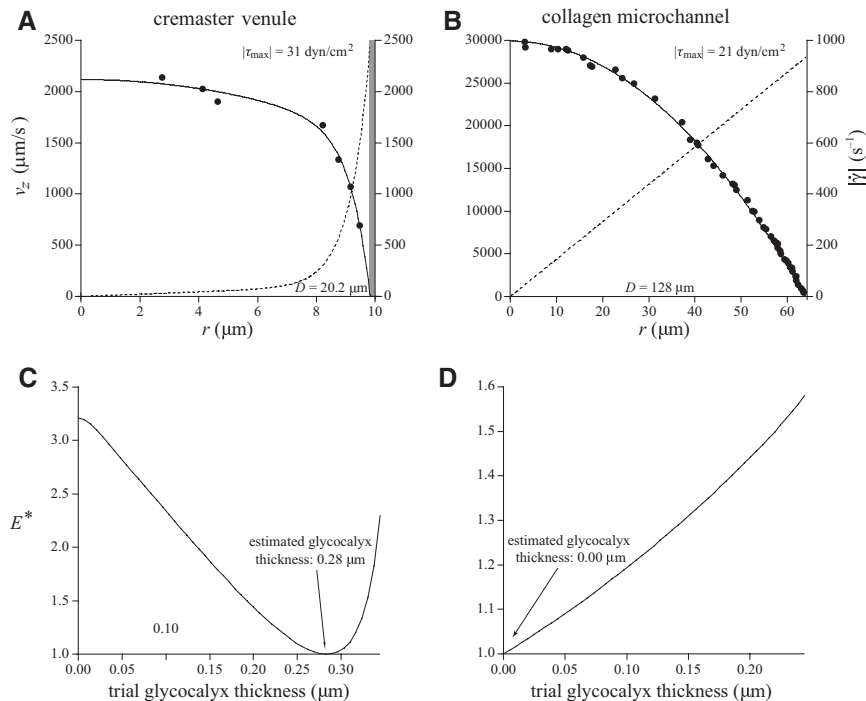


**Figure 2.** Representative fluorescent  $\mu$ -PIV data (dots) obtained from a 20- $\mu$ m-diameter mouse cremaster muscle venule in vivo (A) and a 128- $\mu$ m-diameter HUVEC-lined collagen microchannel cultured under standard cell culture conditions before treatment with hyaluronidase (B). A monotonic filter has been applied (see Materials and Methods) to filter out data not in the midsagittal plane of the venule or collagen microchannel. Superimposed on the  $\mu$ -PIV data in A and B are the axisymmetric velocity distributions,  $v_z(r)$  (solid curve, left axis). Shear rate distributions (dashed curve, right axis) are also shown in A and B. Note the nonlinear variation in  $\dot{\gamma}$  that arises in the venule resulting from the axial concentration of red blood cells that occurs in the microcirculation.<sup>12,13</sup> Variations C and D in the normalized least squares error,  $E^*$ , associated with the fit to the  $\mu$ -PIV data shown, respectively, in A and B as a function of the trial glyocalyx thickness. The estimated hydrodynamically relevant glyocalyx thickness corresponds to the minimum value of  $E^*$  found among all trial values considered, which was found to be  $\approx 0.3 \mu\text{m}$  for the venule in A and  $0 \mu\text{m}$  for the collagen microchannel in B.

treatment, the mean hydrodynamically relevant thickness was found not to be significantly different from  $0 \mu\text{m}$  ( $0.02 \pm 0.04 \mu\text{m}$ , 0.00 to  $0.11 \mu\text{m}$ ). (Because hyaluronidase is preferential but not specific to HA, the present data do not imply that HA is a constituent of the endothelial glyocalyx in vivo. The biomolecular identity of what is actually being cleaved by hyaluronidase remains to be established.) In HUVEC-lined collagen microchannels ( $131 \pm 10 \mu\text{m}$ , 113 to  $150 \mu\text{m}$  diameter), the mean hydrodynamically relevant thickness of the EC surface layer was found not to be significantly different from  $0 \mu\text{m}$  either before ( $0.03 \pm 0.04 \mu\text{m}$ , 0.00 to  $0.10 \mu\text{m}$ ) or after ( $0.02 \pm 0.04 \mu\text{m}$ , 0.00 to  $0.12 \mu\text{m}$ ) hyaluronidase treatment (Figure 3). Experiments were conducted at both room temperature ( $22^\circ\text{C}$  to  $24^\circ\text{C}$ ) and body temperature ( $36^\circ\text{C}$  to  $38^\circ\text{C}$ ), but this variable had no significant effect on the hydrodynamically relevant thickness of the EC glyocalyx either in vivo or in vitro (supplemental Figure XI). The maximum shear stress,  $|\tau_{\text{max}}|$ , averaged over all 58 experiments in HUVEC-lined collagen microchannels was found to be  $12 \pm 3 \text{ dyn/cm}^2$  (4 to  $21 \text{ dyn/cm}^2$ ) compared with the average value of  $23 \pm 23 \text{ dyn/cm}^2$  (4 to  $103 \text{ dyn/cm}^2$  over all 34 venules analyzed).

To test our ability to resolve a hydrodynamically relevant layer on the luminal HUVEC surface of our collagen microchannels, and to attempt to constitute a glycosaminoglycan layer on ECs in vitro, we conducted another series of experiments that were designed to emulate the in vivo glyocalyx reconstitution experiments of Henry and Duling.<sup>35</sup> In particular, we added a physiological dose of HA and CS to the culture media ( $0.1 \mu\text{g/mL}$ ), collected  $\mu$ -PIV data, then treated with hyaluronidase to degrade HA, collected  $\mu$ -PIV data again, then added a pharmacological dose of HA and CS ( $0.2 \text{ mg/mL}$ ), and collected  $\mu$ -PIV data once more. Analysis of these  $\mu$ -PIV data sets revealed that the mean hydrodynam-

ically relevant thickness of the EC surface layer was not significantly different from  $0 \mu\text{m}$  in microchannels cultured with a physiological dose of HA and CS before ( $0.07 \pm 0.16 \mu\text{m}$ , 0.00 to  $0.45 \mu\text{m}$ ) or after ( $0.02 \pm 0.04 \mu\text{m}$ , 0.00 to  $0.15 \mu\text{m}$ ) hyaluronidase treatment but was significantly different from  $0 \mu\text{m}$  after ( $0.21 \pm 0.27 \mu\text{m}$ , 0.00 to  $0.63 \mu\text{m}$ ,  $P < 0.05$ ) the pharmacological dose of HA and CS was added (Figure 3). Thus, our HUVEC-lined collagen microchannels do indeed provide sufficient resolution to detect a hydrodynamically relevant EC surface-bound glycosaminoglycan layer when such a layer is present. We are not suggesting that the occasional surface-bound macromolecular layer thus found is indicative of the glyocalyx per se, but rather we look on these experiments as positive control that our in vitro system does indeed have the sensitivity and resolution necessary to detect hydrodynamically relevant surface chemistry of the same order of magnitude as the glyocalyx that we see in vivo.

To test whether the glyocalyx defect reported here in the HUVEC culture model extends to BAECs, we performed  $\mu$ -PIV experiments in BAEC-lined collagen microchannels ( $100 \pm 9 \mu\text{m}$ , 88 to  $109 \mu\text{m}$  diameter) before and after hyaluronidase treatment. In contrast to our HUVEC-lined microchannels, however, the BAECs frequently protruded well into the lumen of the microchannel, often extending into the lumen by  $>20\%$  of the radius of the microchannel (compare Figure 1 and supplemental Figure XII). These undulations in the luminal surface led to significant asymmetries in the velocity profile, which in turn limited our analysis to near-wall  $\mu$ -PIV (restricted to microspheres within  $3 \mu\text{m}$  of the luminal BAEC surface)<sup>11</sup> rather than the full-field analysis<sup>12</sup> that we used in HUVEC-lined microchannels and venules. Despite this morphology, the BAECs gave no indication of peeling off of the collagen even after four days

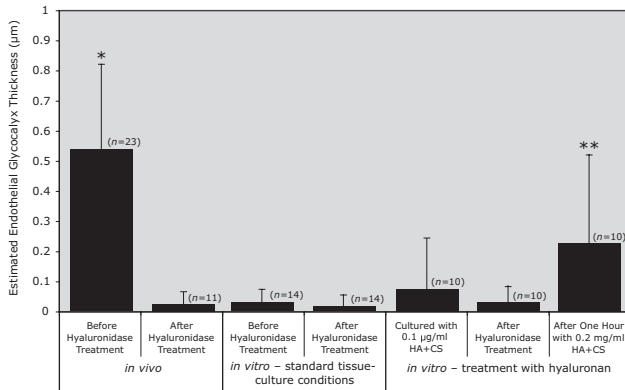


**Figure 3.** Estimates of the mean hydrodynamically relevant thickness of the EC surface layer in cremaster muscle venules in vivo and HUVEC-lined microchannels in vitro. In mouse cremaster muscle venules the mean hydrodynamically relevant EC surface layer thickness was found to be  $\approx 0.52 \mu\text{m}$  before hyaluronidase treatment and was found not to be significantly different from  $0 \mu\text{m}$  after treatment with  $50 \text{ U/mL}$  hyaluronidase for 1 hour. In contrast, the mean hydrodynamically relevant EC surface layer thickness on HUVECs grown to confluence under standard cell culture conditions on the luminal surface of collagen microchannels was found not to be significantly different from  $0 \mu\text{m}$  before or after hyaluronidase treatment. The mean hydrodynamically relevant EC surface layer thickness on HUVECs cultured with a physiological dose ( $0.1 \mu\text{g/mL}$ ) of HA and CS added to otherwise standard cell culture media was found not to be significantly different from  $0 \mu\text{m}$  before or after hyaluronidase treatment. However, when these cells were treated with a pharmacological dose ( $0.2 \text{ mg/mL}$ ) of HA and CS (to both quench the hyaluronidase and provide a large pool of HA and CS complexes to bind to the EC surface), the mean hydrodynamically relevant EC surface layer thickness was found to be  $\approx 0.21 \mu\text{m}$ . \* $P < 0.0005$ , \*\* $P < 0.05$ .

at confluence (whereas all  $\mu$ -PIV experiments were done after 1 day at confluence). A 2-color fluorescence Live/Dead Viability/Cytotoxicity kit (Invitrogen) confirmed the viability of the BAECs (supplemental Figure XIII). As with HUVECs, the mean hydrodynamically relevant thickness of the EC surface layer in 5 BAEC-lined microchannels was found not to be significantly different from  $0 \mu\text{m}$  either before ( $0.02 \pm 0.04 \mu\text{m}$ ,  $0.00$  to  $0.08 \mu\text{m}$ ) or after ( $0 \mu\text{m}$  for all 5 microchannels) hyaluronidase treatment (supplemental Figure XIV). In cremaster muscle venules, the hydrodynamically relevant glycocalyx thickness found using near-wall  $\mu$ -PIV before hyaluronidase treatment ( $0.52 \pm 0.42 \mu\text{m}$ ,  $0.16$  to  $1.14 \mu\text{m}$ ) was significantly different from  $0 \mu\text{m}$  ( $P < 0.0005$ ) but was not significantly different from that obtained using full-field  $\mu$ -PIV ( $0.52 \pm 0.28 \mu\text{m}$ ,  $0.16$  to  $1.14 \mu\text{m}$ ). As with full-field  $\mu$ -PIV analysis, the hydrodynamically relevant thickness of the glycocalyx using near-wall  $\mu$ -PIV analysis in venules after hyaluronidase treatment was found not to be significantly different from  $0 \mu\text{m}$  ( $0.03 \pm 0.06 \mu\text{m}$ ,  $0.00$  to  $0.17 \mu\text{m}$ ).

Through detailed analysis of the hydrodynamic drag near the EC surface, coupled with  $\mu$ -PIV data obtained in mouse cremaster muscle venules in vivo and in EC-lined collagen microchannels in vitro, we have identified a fundamental defect in EC culture models that extends across 2 prominently used cell types: HUVECs and BAECs. The complete absence in these 2 cell types of a hydrodynamically relevant endothe-

lial glycocalyx under standard cell culture conditions likewise implies a deficiency in cell surface chemistry that casts doubt on the applicability of these EC culture models to many of the vascular functions and pathologies that they have been used to study.<sup>1-9,43</sup> A recent study by Jacob et al<sup>33</sup> found a similar deficiency in the glycocalyx of fixed HUVECs, which the present results now extend to live HUVECs while in the presence of a physiologically typical hydrodynamic shear stress environment. Similar studies need to be conducted using other cell types and under nonstandard cell culture conditions to determine whether these findings depend on cell type and/or cellular environment. Although these results are biochemically nonspecific, they nevertheless have functional significance for ECs, because the in vivo hydrodynamic properties of the endothelial glycocalyx, which we have shown to be absent in vitro, determine flow and mechanical stress at the EC surface. These hydrodynamic properties in turn influence the manner in which mechanical stress is transduced by ECs, leukocytes interact with inflamed endothelium, and the transport of water and macromolecules is regulated by the vasculature.<sup>44</sup> As such, to adequately capture these processes with an EC-culture model, it will be necessary, if not sufficient, to faithfully reconstruct the hydrodynamic environment at the EC surface in vivo.

### Acknowledgments

Thanks to J. Jiang for providing laboratory and surgical assistance, M.D. Savery for assistance with software development, J. Tien for valuable suggestions and advice, and P. Allen for providing technical assistance with the confocal imaging.

### Sources of Funding

Supported by NIH grant R01-HL076499.

### Disclosures

None.

### References

1. Yang L, Froio RM, Sciuto TE, Dvorak AM, Alon R, Luscinskas FW. ICAM-1 regulates neutrophil adhesion and transcellular migration of TNF-alpha-activated vascular endothelium flow. *Blood*. 2005;106:584-592.
2. Surapishchat J, Hoefen RJ, Pi X, Yoshizumi M, Yan C, Berk BC. Fluid shear stress inhibits TNF-alpha activation of JNK but not ERK1/2 or p38 in human umbilical vein endothelial cells: Inhibitory crosstalk among MAPK family members. *Proc Natl Acad Sci U S A*. 2001;98:6476-6481.
3. Gautam AN, Olofsson M, Herwald H, Iversen LF, Lundgren-Akerlund E, Hedqvist P, Arfors KE, Flodgaard H, Lindbom L. Heparin-binding protein (HBP/CAP37): a missing link in neutrophil-evoked alteration of vascular permeability. *Nat Med*. 2001;7:1123-1127.
4. Tzima E, Irani-Tehrani M, Kiosses WB, Dejiana E, Schultz DA, Engelhardt B, Cao G, DeLisser H, Schwartz MA. A mechanosensory complex that mediates the endothelial cell response to fluid shear stress. *Nature*. 2005;437:426-431.
5. Topper JN, Cai J, Falb D, Gimbrone Jr MA. Identification of vascular endothelial genes differentially responsive to fluid mechanical stimuli: cyclooxygenase-2, manganese superoxide dismutase, and endothelial cell nitric oxide synthase are selectively up-regulated by steady laminar shear stress. *Proc Natl Acad Sci U S A*. 1996;93:10417-10422.
6. McCormick SM, Eskin SG, McIntire LV, Teng CL, Lu CM, Russell CG, Chittur KK. DNA microarray reveals changes in gene expression of shear stressed human umbilical vein endothelial cells. *Proc Natl Acad Sci U S A*. 2001;98:8955-8960.
7. Florian JA, Kosky JR, Ainslie K, Pang Z, Dull RO, Tarbell JM. Heparan sulfate proteoglycan is a mechanosensor on endothelial cells. *Circ Res*. 2003;93:136-142.

8. Thi MM, Tarbell JM, Weinbaum S, Spray DC. The role of the glycocalyx in reorganization of the actin cytoskeleton under fluid shear stress: a "bumper-car" model. *Proc Natl Acad Sci U S A*. 2004;101:16483–16488.
9. Theriault A, Chao JT, Gapor A. Tocotrienol is the most effective vitamin E for reducing endothelial expression of adhesion molecules and adhesion to monocytes. *Atherosclerosis*. 2002;160:21–30.
10. Vink H, Duling BR. Identification of distinct luminal domains for macromolecules, erythrocytes, and leukocytes within mammalian capillaries. *Circ Res*. 1996;79:581–589.
11. Smith ML, Long DS, Damiano ER, Ley K. Near-wall micro-PIV reveals a hydrodynamically relevant endothelial surface layer in venules in vivo. *Biophys J*. 2003;85:637–645.
12. Damiano ER, Long DS, Smith ML. Estimation of viscosity profiles using velocimetry data from parallel flows of linearly viscous fluids: application to microvascular haemodynamics. *J Fluid Mech*. 2004;512:1–19.
13. Long DS, Smith ML, Pries AR, Ley K, Damiano ER. Microviscometry reveals reduced blood viscosity and altered shear rate and shear stress profiles in microvessels after hemodilution. *Proc Natl Acad Sci U S A*. 2004;101:10060–10065.
14. Damiano ER, Duling BR, Ley K, Skalak TC. Axisymmetric pressure-driven flow of rigid pellets through a cylindrical tube lined with a deformable porous wall layer. *J Fluid Mech*. 1996;314:163–189.
15. Damiano ER. The effect of the endothelial cell glycocalyx on the motion of red blood cells through capillaries. *Microvasc Res*. 1998;55:77–91.
16. Secomb TW, Hsu R, Pries AR. A model for red blood cell motion in glycocalyx-lined capillaries. *Am J Physiol*. 1998;274:H1016–H1022.
17. Feng J, Weinbaum S. Lubrication theory in highly compressible porous media: the mechanics of skiing, from red cells to humans. *J Fluid Mech*. 2000;422:281–317.
18. Secomb TW, Hsu R, Pries AR. Motion of red blood cells in a capillary with an endothelial surface layer: effect of flow velocity. *Am J Physiol*. 2001;281:H629–H636.
19. Damiano ER, Stace TM. A mechano-electrochemical model of radial deformation of the capillary glycocalyx. *Biophys J*. 2002;82:1153–1175.
20. Weinbaum S, Zhang X, Han Y, Vink H, Cowin SC. Mechanotransduction and flow across the endothelial glycocalyx. *Proc Natl Acad Sci U S A*. 2003;100:7988–7995.
21. Damiano ER, Stace TM. Flow and deformation of the capillary glycocalyx in the wake of a leukocyte. *Phys Fluids*. 2005;17:031509-1–031509-17.
22. Han Y, Weinbaum S, Spaan JAE, Vink H. Large-deformation analysis of the elastic recoil of fibre layers in a Brinkman medium with application to the endothelial glycocalyx. *J Fluid Mech*. 2006;554:217–235.
23. Henry CBS, Duling BR. TNF-alpha increases entry of macromolecules into luminal endothelial cell glycocalyx. *Am J Physiol*. 2000;279:H2815–H2823.
24. Mulivor AW, Lupowsky HH. Role of glycocalyx in leukocyte-endothelial cell adhesion. *Am J Physiol*. 2002;283:H1282–H1291.
25. Mulivor AW, Lupowsky HH. Inflammation- and ischemia-induced shedding of venular glycocalyx. *Am J Physiol*. 2004;286:H1672–H1680.
26. Platts SH, Lindan J, Duling BR. Rapid modification of the glycocalyx caused by ischemia-reperfusion is inhibited by adenosine A2A receptor activation. *Am J Physiol*. 2003;284:H2360–H2367.
27. Platts SH, Duling BR. Adenosine A3 receptor activation modulates the capillary endothelial glycocalyx. *Circ Res*. 2004;94:77–82.
28. Rubio-Gayosso I, Platts SH, Duling BR. Reactive oxygen species mediate modification of glycocalyx during ischemia-reperfusion injury. *Am J Physiol*. 2006;290:H2247–H2256.
29. Secomb TW, Hsu R, Pries AR. Effect of the endothelial surface layer on transmission of fluid shear stress to endothelial cells. *Biorheology*. 2001;38:143–150.
30. Squire JM, Chew M, Nneji G, Neal C, Barry J, Michel C. Quasi-periodic substructure in the microvessel endothelial glycocalyx: a possible explanation for molecular filtering? *J Struct Biol*. 2001;136:239–255.
31. Adamson RH, Lenz JF, Zhang X, Adamson GN, Weinbaum S, Curry FE. Oncotic pressures opposing filtration across non-fenestrated rat microvessels. *J Physiol*. 2004;557:889–907.
32. van den Berg BM, Vink H, Spaan JAE. The endothelial glycocalyx protects against myocardial edema. *Circ Res*. 2003;92:592–594.
33. Jacob M, Rehm M, Loetsch M, Paul JO, Bruegger D, Welsch U, Conzen P, Becker BF. The endothelial glycocalyx prefers albumin for evoking shear stress-induced, nitric oxide-mediated coronary dilatation. *J Vasc Res*. 2007;44:435–443.
34. Levick JR. Flow through interstitium and other fibrous matrices. *Q J Exp Physiol*. 1987;72:409–437.
35. Henry CBS, Duling BR. Permeation of the luminal capillary glycocalyx is determined by hyaluronan. *Am J Physiol*. 1999;279:H508–H514.
36. Chrobak KM, Potter DR, Tien J. Formation of perfused, functional microvascular tubes in vitro. *Microvasc Res*. 2006;185:185–196.
37. Normand KE. An effective and economical solution for digitizing and analyzing video recordings of the microcirculation. *Microcirculation*. 2001;8:243–249.
38. Ley K, Bullard DC, Arbones ML, Bosse R, Vestweber D, Tedder TF, Beaudet AL. Sequential contribution of L- and P-selectin to leukocyte rolling in vivo. *J Exp Med*. 1995;181:669–675.
39. Cokelet GR. Viscometric, in vitro, and in vivo blood viscosity relationships: how are they related? *Biorheology*. 1999;36:343–358.
40. Lew HS, Fung YC. Entry flow into blood vessels at arbitrary Reynolds number. *J Biomech*. 1970;3:23–38.
41. Goldman AJ, Cox RG, Brenner H. Slow viscous motion of a sphere parallel to a plane wall—II Couette flow. *Chem Eng Sci*. 1967;22:653–660.
42. Damiano ER, Long DS, El-Khatib FH, Stace TM. On the motion of a sphere in a Stokes flow parallel to a Brinkman half-space. *J Fluid Mech*. 2004;500:75–101.
43. Yao Y, Rabadzay A, Dewey CF. Glycocalyx modulates the motility and proliferative response of vascular endothelium to fluid shear stress. *Am J Physiol*. 2007;293:H1023–H1030.
44. Weinbaum S, Tarbell JM, Damiano ER. The structure and function of the endothelial glycocalyx layer. *Annu Rev Biomed Eng*. 2007;9:121–167.